AD-A193 361 METHOD FOR LOCATING A SMALL MAGNETIC OBJECT IN THE HUMAN BODY(U) NEW YORK UNIV N Y L KAUFMAN ET AL 29 FEB 88 AFOSR-TR-88-0370 F49620-85-K-0004 1/1

UNCLASSIFIED F/G 6/5 NL

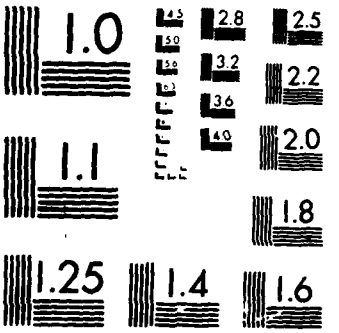
1.0
1.1
1.25
1.4
1.6
1.8
2.0
2.2
2.5
2.8
3.2
3.6
4.0
4.5
5.0
5.6
6.3

SECURITY CLASSIFICATION OF THIS PAGE

DTIC FILE COPY

REPORT DOCUMENTATION PAGE

Form Approved OMB No. 0704-0188

1a. REPORT SECURITY CLASSIFICATION: unclassified	1b. RESTRICTIVE MARKINGS
	3. DISTRIBUTION/AVAILABILITY OF REPORT: Approved for public release distribution unlimited
AD-A193 361 S)	5. MONITORING ORGANIZATION REPORT NUMBER(S): AFOSR-TR- 88-0370
6a. NAME OF PERFORMING ORGANIZATION: New York University; 6b. OFFICE SYMBOL (If applicable):	7a. NAME OF MONITORING ORGANIZATION: Air Force Office of Scientific Research
6c. ADDRESS (City, State, and ZIP Code): Departments of Psychology and Physics, 4 Washington Place - New York, NY 10003	7b. ADDRESS (City, State, and ZIP Code): Building 410, Bolling AFB, DC 20332-6448
8a. NAME OF FUNDING/SPONSORING ORGANIZATION: AFSOR; 8b. OFFICE SYMBOL (If applicable): NL	9. PROCUREMENT INSTRUMENT IDENTIFICATION NUMBER: F49620-85-K-0004
8c. ADDRESS (City, State, and ZIP Code): Building 410, Bolling AFB, DC 20332	10. SOURCE OF FUNDING NUMBERS: PROGRAM ELEMENT NO. 61102F; PROJECT NO. 2313; TASK NO A4; WORK UNIT ACCESSION NO.

11. TITLE (Include Security Classification)
METHOD FOR LOCATING A SMALL MAGNETIC OBJECT IN THE HUMAN BODY

12. PERSONAL AUTHOR(S)
Lloyd Kaufman, Samuel J. Williamson, Risto J. Ilmoniemi, Harold Weinberg, and Arthur D. Boy

13a. TYPE OF REPORT	13b. TIME COVERED	14. DATE OF REPORT (Year, Month, Day)	15. PAGE COUNT
Publication	FROM _____ TO _____	Feb. 29, 1988	15

16. SUPPLEMENTARY NOTATION

17. COSATI CODES			18. SUBJECT TERMS (Continue on reverse if necessary and identify by block number)
FIELD	GROUP	SUB-GROUP	SQUID-SURGERY; X-RAY; MAGNETIC FIELDS

19. ABSTRACT (Continue on reverse if necessary and identify by block number)

A piece of a thin acupuncture needle lodged under the right scapula of a patient could not be found in surgical procedures accompanied by studies of 30 standard X-ray images. To locate it, we mapped the magnetic field component normal to a plane lying above the object, using a superconducting quantum interference device (SQUID). Assuming that the needle could be modelled as a magnetic dipole, we were able to infer its lateral position, depth, orientation, and magnetic moment. With this information, directed CT scans, high-resolution X-ray films, and the subsequent surgical removal of the needle proved that it could be located in the body with an accuracy of about three millimeters.

20. DISTRIBUTION/AVAILABILITY OF ABSTRACT	21. ABSTRACT SECURITY CLASSIFICATION
☒ UNCLASSIFIED/UNLIMITED ☒ SAME AS RPT ☐ DTIC USERS	unclassified
22a. NAME OF RESPONSIBLE INDIVIDUAL: Dr. Alfred R. Fregly	22b. TELEPHONE (Include Area Code): 202-767-5024; 22c. OFFICE SYMBOL: NL

DD Form 1473, JUN 86 — Previous editions are obsolete. — SECURITY CLASSIFICATION OF THIS PAGE

16 MAR 1988

To be published in
IEEE Transactions of Biomedical Engineering, 1988

Method for Locating a Small Magnetic Object in the Human Body

RISTO J. ILMONIEMI, SAMUEL J. WILLIAMSON, MEMBER, IEEE, LLOYD KAUFMAN, HAROLD WEINBERG, AND ARTHUR D. BOYD

Abstract - A piece of a thin acupuncture needle lodged under the right scapula of a patient could not be found in surgical procedures accompanied by studies of 30 standard X-ray images. To locate it, we mapped the magnetic field component normal to a plane lying above the object, using a superconducting quantum interference device (SQUID). Assuming that the needle could be modelled as a magnetic dipole, we were able to infer its lateral position, depth, orientation, and magnetic moment. With this information, directed CT scans, high-resolution X-ray films, and the subsequent surgical removal of the needle proved that it could be located in the body with an accuracy of about three millimeters.

This work was supported in part by National Institutes of Health grant NSI9463-03, Air Force Office of Scientific Research grant F49620-85-K-0004, and the Emil Aaltonen Foundation (Finland).

Risto J. Ilmoniemi, Samuel J. Williamson, and Lloyd Kaufman are with the Neuromagnetism Laboratory, Departments of Physics and Psychology, New York University, New York, NY 10003, U.S.A. The permanent address of Risto J. Ilmoniemi is the Low Temperature Laboratory, Helsinki University of Technology, 02150 Espoo, Finland.

Harold Weinberg is with the Department of Neurology, and Arthur D. Boyd is with the Department of Surgery, New York University Medical Center, 550 First Avenue, New York, NY 10016, U.S.A.

I. INTRODUCTION

We report the successful application of a technique to detect and locate with millimeter precision magnetic objects in the human body. This procedure may be advantageous for applications as localizing magnetic objects causing discomfort, with the prospect of subsequent surgical removal, and for detecting magnetic objects prior to exposure to strong magnetic fields as when recording data for MR images.[1] The object in our study was a portion of an acupuncture needle, lodged under the right scapula of a patient, but the technique has more general applicability to objects in other locations, so long as the magnetic field they produce is sufficiently strong. The technique is to map the magnetic field normal to a plane above the object and from the measured field pattern deduce the lateral position, depth, orientation, and magnetic moment of the equivalent magnetic dipole.

The instrument having the highest sensitivity for low-frequency measurements of magnetic field is the SQUID (Superconducting QUantum Interference Device), commonly used for studies of the weak magnetic fields associated with the human body.[2] The superconducting sensing elements of the SQUID magnetometer must be maintained in a vacuum-insulated container, or dewar, that contains liquid helium for low-temperature operation (see Figure 1). The magnetic field is sensed by a detection coil that is part of a closed superconducting loop, which has the property that when a field is applied to the detection coil an electrical current is set up in the loop. A part of this loop is coupled magnetically to the SQUID. The SQUID's response is registered as an output voltage from room temperature electronics. The inherent sensitivity of such a field sensor is about 20×10^{-15} tesla for a 1-hertz bandwidth. By comparison, the earth's steady magnetic field is about 70×10^{-6} tesla. However, the sensitivity of the method for measurements of steady fields is limited by low-frequency variations of the ambient field. The detection coil of our sensor had the geometry of a second-order gradiometer to reduce its sensitivity to ambient noise fields, which are comparatively uniform in space.[1]

A commercial system of this kind, which is actually designed for measurements of the magnetic field of the human brain,[3] was applied to study of the steady field from a magnetized object in the body. The object was a portion of an acupuncture needle that had fractured during treatment and was lodged in the upper right region of the patient's back, near the region where he felt pain. One X-ray image taken prior to a surgical procedure at another institution for removal of the needle showed evidence of a needle, but it was not found during two operations, nor was it seen in 29 further X-ray images. For this reason a magnetic study was sought to determine whether the needle might still be in place.

A-1

1. Ambient noise depends on the location of the measurement. The ones reported here were conducted on the 9th floor of a building in Manhattan, some 11 storeys above a subway line that is the major source of magnetic noise. No magnetic shielding was used, but to reduce ambient noise the detection coil was a second-order gradiometer with a baseline between adjacent coils of 4.0 cm, and a diameter of 1.5 cm for each coil.

To map the magnetic field pattern over the back, our patient lay prone on a firm bed, which was supported by rollers. During a scan, the bed was smoothly moved under the magnetometer, while its position was monitored by the voltage from a linear potentiometer attached to the bed. Each linear scan was performed three or more times to assure reliability; upon completion of a set of scans, the bed was displaced laterally by 2 cm and another set of scans was recorded. Figure 2 illustrates the variation of field with position over the patient's back for five adjacent longitudinal scans. A pointer mounted on the dewar holder enabled us to reference positions across the plane of measurement to positions on the posterior torso. Data were recorded in the bandwidth 1-45 Hz, with the subject being moved under the coil at a rate of about 0.15 m/s. The only significant source of noise in these traces is a slow variation of the ambient field, which produces a drift of the baseline. These data may be compared with field patterns produced by magnetic dipoles having different orientations, as illustrated in Figure 3. For purposes of locating a magnetic object, representing the magnetic field of the object by that of a magnetic dipole is justified if the linear dimensions of the object are small in comparison with the distance separating it from the detection coil of the sensor.

Analysis of the data was carried out by two methods. The first depended upon identifying the positions of the positive and negative field extrema, as well as determining the values of the field at these extrema. This information is sufficient to determine the three position coordinates of the dipole, the two angles specifying its orientation, and the moment specifying its strength. A second method was based on using a computer routine to determine the least-squares fit to the field pattern. The deduced positions of the dipole determined by the two methods agreed to better than 3 mm, with the least-squares method being the more accurate. If the position is determined relative to reference points marked on the skin, a much greater error can be introduced from movement of the skin relative to underlying tissue. In such cases, either method of determining the source may be satisfactory.

II. DIPOLE LOCATION BASED ON FIELD EXTREMA

Our analysis is based on the standard formula [4] for the magnetic field produced by a magnetic dipole. The signal produced in the gradiometer was computed from the component of the field parallel to the gradiometer's axis at each of the three coils. Figure 3 shows that the distance separating the locations of signal extrema across the flat surface and the relative magnitudes of the extrema depend on the dipole's inclination α with respect to the measurement plane. Figure 4 illustrates the field variation along the line joining the two field extrema for the case when the dipole is inclined by 20 deg. Various characteristics of the field pattern are also defined.

The dipole lies directly below the axis of mirror symmetry of the pattern. This determines the first position coordinate. Its projection on the measurement plane points from the minimum of the field pattern towards its maximum, establishing its azimuth. The ratio of the two field extrema determines the inclination of the dipole with respect to the measurement plane. This is shown explicitly in Figure 5. In the limit when α approaches 90 deg the negative extremum no longer represents a point on the plane but

has the form of a circle centered on the positive extremum.

The distance D between field extrema for a given inclination α determines the dipole's depth d, as well as the shift of its position with respect to the midpoint between extrema. With these parameters established, the difference ΔB between the minimum and maximum field values (i.e., the sum of the magnitudes of the two field extrema) together with the relation

$$M = 4\pi K \mu_o^{-1} \Delta B d^3 \quad (1)$$

determines the strength M of the dipole's moment, where $\mu_o = 4\pi \times 10^{-7}$ H·m^{-1} is the permeability of free space. This expression can be derived from dimensional arguments, with the prefactor of 4π included so that the value of the dimensionless scaling factor K lies between 0.1 and 1. Figure 6 shows how the positional parameters d and Δx as well as the scaling factor K are determined by D and ΔB. Then Eq. (1) can be used to compute the dipole's strength M.

We emphasize that the curves in Figs. 5 and 6 have been computed for a magnetometer that measures the normal component of the magnetic field across a plane. A similar procedure could be used to compute curves for any gradiometer. In such a case, however, it might well be more convenient to carry out a least-squares fit as explained next.

III. DIPOLE LOCATION FROM A LEAST-SQUARES FIT

The second method for locating a dipole is based on a least-squares fit to the data. Values of the measured field were read from the curves of Figure 2 at points on a rectangular grid, with 25 mm separating points along each scan and 2 cm separating points on adjacent scans. These data were then used by a least-squares fitting routine to determine the six dipole parameters that produce the best matching field in a least-squares sense to the 40 measured values. Initial estimates for the dipole parameters were obtained from the preceding method based on the locations and strengths of the signal extrema.

Several verification tests were carried out with a 15-mm length of an acupuncture needle mounted on the subject bed, so that its position and orientation could be directly measured, confirmed the accuracy of this analysis. In fact, it was found that instrumental noise caused an error of only 0.8 mm in position.

The main source of error in our procedure was caused by the fact that changes in a patient's posture may move the skin laterally with respect to the underlying tissue. The measurement procedure with our patient was repeated over several weeks, with the patient placed in approximately the same position; yet the last three measurements showed a systematic caudal shift of about 5 mm. It is not known whether this variability between different days was due to errors in positioning the patient, or whether the needle had moved between measurements. The dipole was deduced to lie at a depth of about 28 mm beneath the skin and was tipped by about 10 deg from being parallel to the overlying skin. Its moment was roughly 10^{-6} A·m^2. This moment is equivalent to a cubic

volume of saturated iron of about 0.1 mm on a side. The surface position of the source was approximately 3 cm caudal to the incision made during the earlier surgical procedure.

The position indicated by the magnetic analysis was used to determine where CT scans should be made, in an attempt to confirm the presence of the needle. Transverse scans through the thorax were obtained through the predicted location at 3-mm displacements longitudinally (Figure 7). A small (1-2 picture elements) high-density feature was evident in the intercostal space between the fifth and sixth ribs, at the predicted depth and lateral position. Based on this information, a surgical procedure was scheduled. On the morning of the procedure, magnetic scanning was repeated with the subject prone and right arm raised above the head, mimicing the position to be assumed during surgery so that the deduced position could most accurately be related to marks placed on the skin. Subsequently, a high-resolution X-ray film was obtained for a frontal cross section of the upper right thorax, and it showed the needle curved at the lateral position indicated by the magnetic analysis. CT scans taken through and near the magnetically deduced position again confirmed the presence of the needle at the predicted depth.

A surgical procedure was conducted with the incision made directly above the position indicated by the magnetic and X-ray studies. As soon as the depth of the incision was about 25 mm, the needle was observed in a curved configuration within the intercostal space between the fifth and sixth ribs, and it was removed.

We have demonstrated that magnetic measurements of the field pattern above a relatively small object can be analyzed to deduce the parameters for an equivalent magnetic dipole representing the magnetic properties of the source. The object in this case was sufficiently large (0.2 mm diameter, 15 mm length) that confirmation could be obtained with CT scans, using the original magnetic localization to indicate where the scan should be taken. The magnetic method itself is non-invasive and involves no discomfort for the patient. The accuracy of the procedure depends on the strength of the detected field in comparison with the ambient noise and inherent noise in the sensor. For measurements with our passband from 1 to 45 Hz, the latter is about 150 fT, corresponding to a magnetic moment at a distance of 4 cm from the sensor of approximately 10^{-10} $A \cdot m^2$.

It is worth noting that this same technique can be employed when the foreign object is not magnetic, but is strongly paramagnetic. By applying an ac field to the subject, a magnetometer such as that used in this study may detect the paramagnetic response of the foreign object at the frequency of the applied field. These responses can then be mapped just as we mapped the field of the magnetic object in this study, and the position of the embedded object can be determined with similar efficacy.[5]

REFERENCES

[1] E.J. Finn, G. Di Chiro, R.A. Brooks, S. Sato, "Ferromagnetic materials in patients: detection before MR imaging," *Radiology* vol. 156, pp 139-141, 1985.

[2] S.J. Williamson, G.-L. Romani, L. Kaufman, I. Modena, Eds., *Biomagnetism: An Interdisciplinary Approach*, New York: Plenum Press, 1983.

[3] Biomagnetic Technologies, Inc., 4174 Sorrento Valley Blvd., San Diego, CA 92121.

[4] B.I. Bleaney and B. Bleaney, *Electricity and Magnetism*, Oxford: Oxford University Press, 1983, pp. 123-124.

[5] C.M. Bastuscheck, S.J. Williamson, "Technique for measuring the ac susceptibility of the human body or other large objects," *J. Appl. Phys.*, vol. 58, pp 3896-3906, 1985.

FIGURE CAPTIONS

Fig. 1. Arrangement of dewar containing the detection coil and SQUID sensor supported above the patient, who is prone on a movable bed. The exact position of the patient with respect to the magnetometer is determined with the pointer whose location and angle are known.

Fig. 2. Observed variation of magnetic field for five longitudinal scans across the region above the magnetic object. Individual scans are separated laterally by 2 cm. Positive field is indicated by upward deflection.

Fig. 3. Isofield contour maps calculated for the second-order gradiometer when a magnetic dipole is inclined from being parallel to the measurement plane by angles of 0, 20, 40, and 90 deg. The distance of the dipole from the measurement plane is assumed to be 9 cm, while the baseline of the gradiometer is 4 cm. The distance between extrema in the 0-deg panel is 7 cm.

Fig. 4. Field variation along the line joining the two field extrema for a magnetic dipole inclined at 20 deg, as detected by the second-order gradiometer. The notation for various features is also defined.

Fig. 5. Inclination angle for various ratios of the field magnitudes at the positions of maximum and minimum field.

Fig. 6. Depth d and position Δx of the dipole relative to the distance D between field extrema, together with the parameter K giving the strength of the dipole, for various ratios of the field magnitudes at the extrema.

Fig. 7. Transverse CT scan of the patient at the longitudinal position predicted by magnetic analysis. The bright feature encircled in black underlying the right scapula, and indicated by the white arrow directed from the lung cavity, presumably is the needle. Other, broader white features are cross sections of ribs. The CT slice thickness is 3 mm. Bright dots on the overlying skin are cross-sections of fiberglass rods used to indicate surface reference positions.

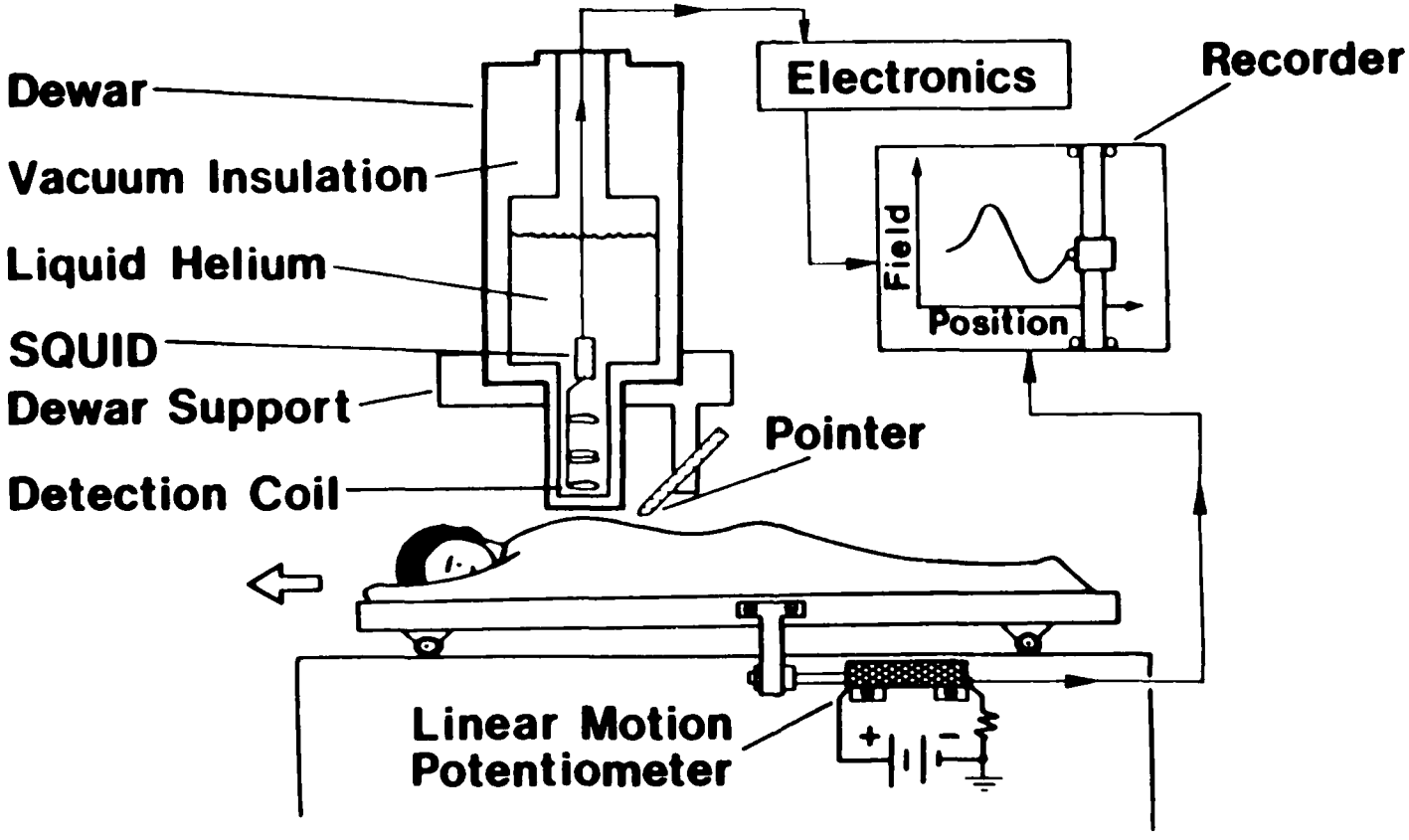
Dewar
Vacuum Insulation
Liquid Helium
SQUID
Dewar Support
Detection Coil
Electronics
Recorder
Field
Position
Pointer
Linear Motion
Potentiometer
+
-

FIGURE 1

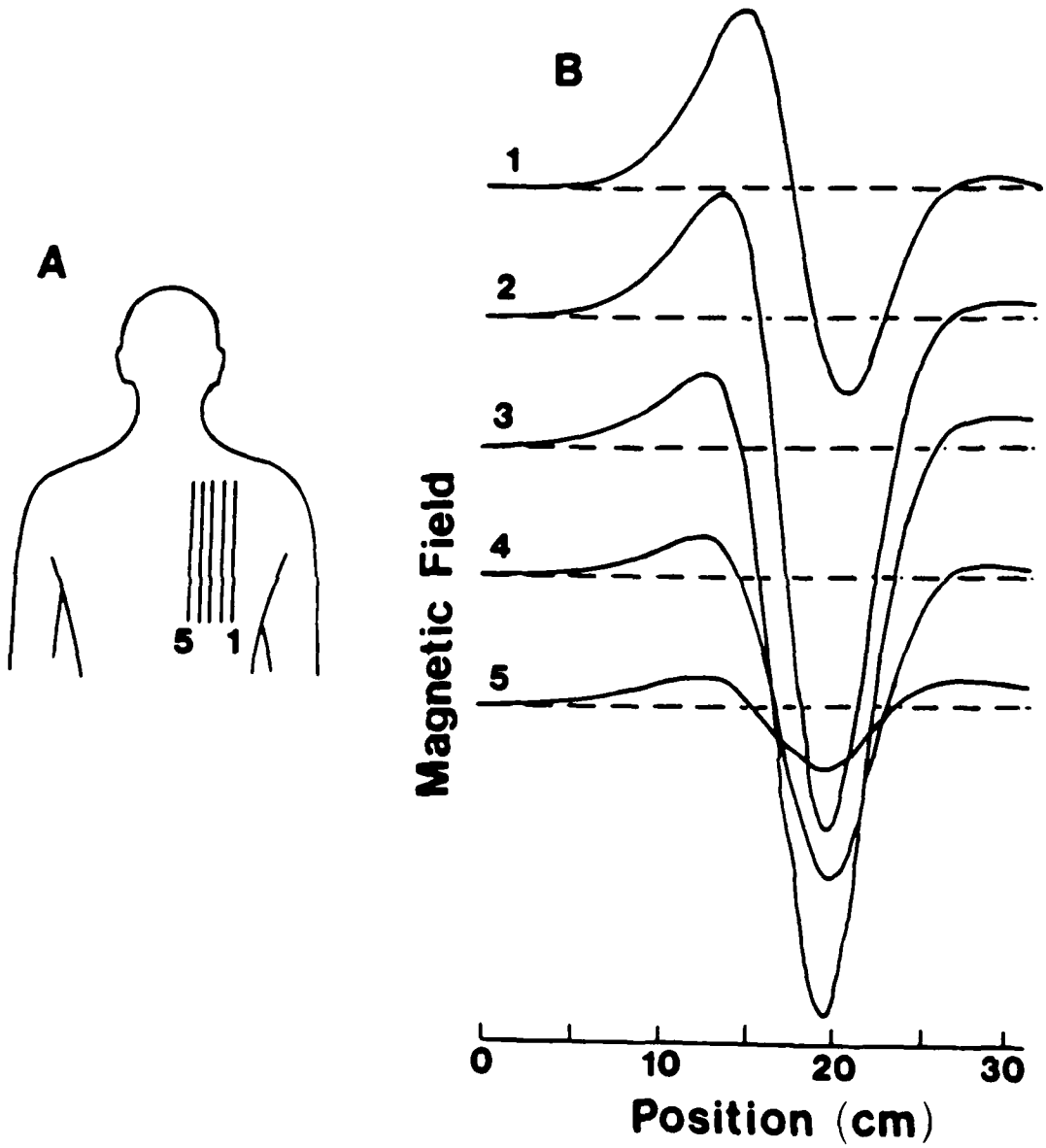

FIGURE 2

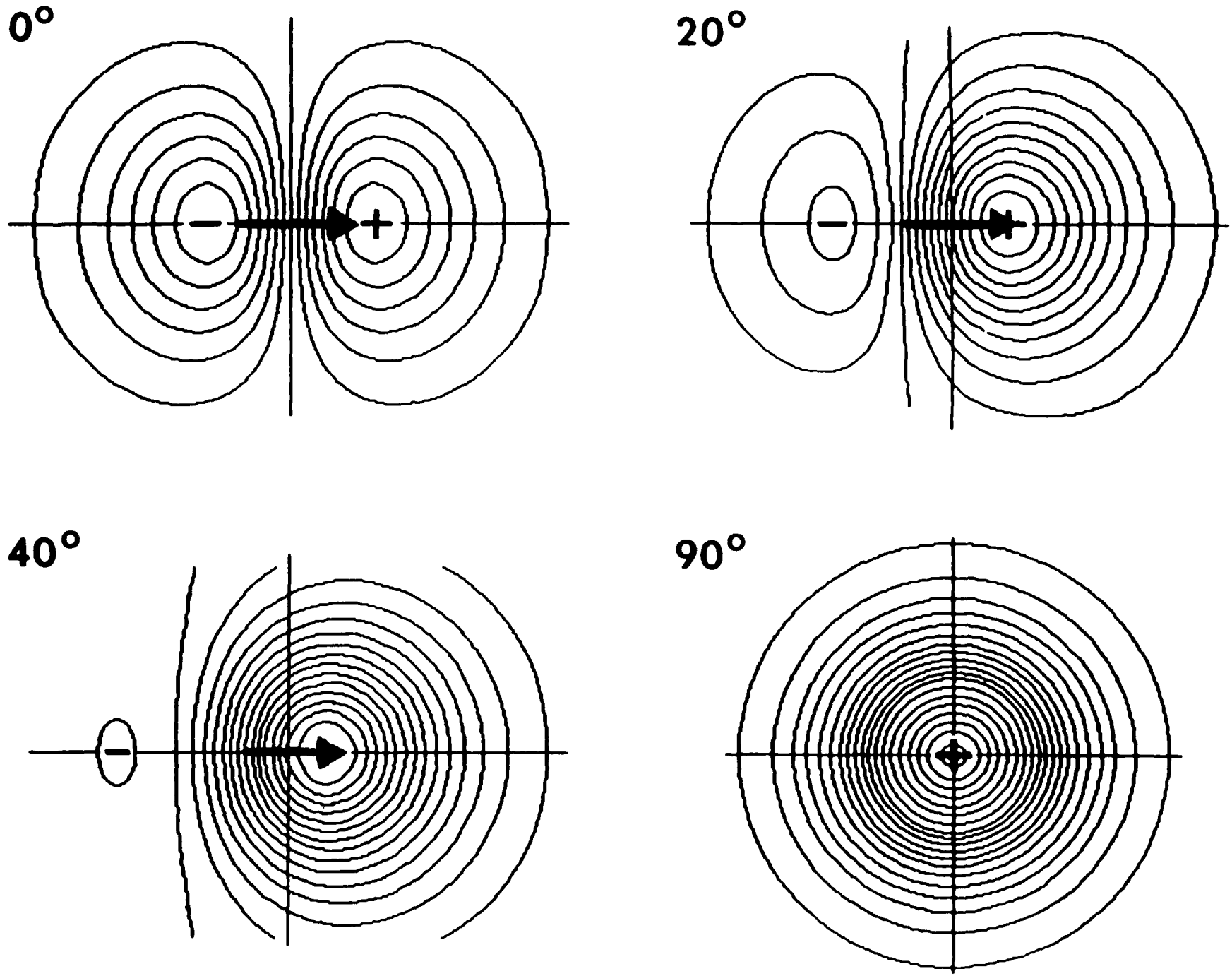
0°
20°
40°
90°

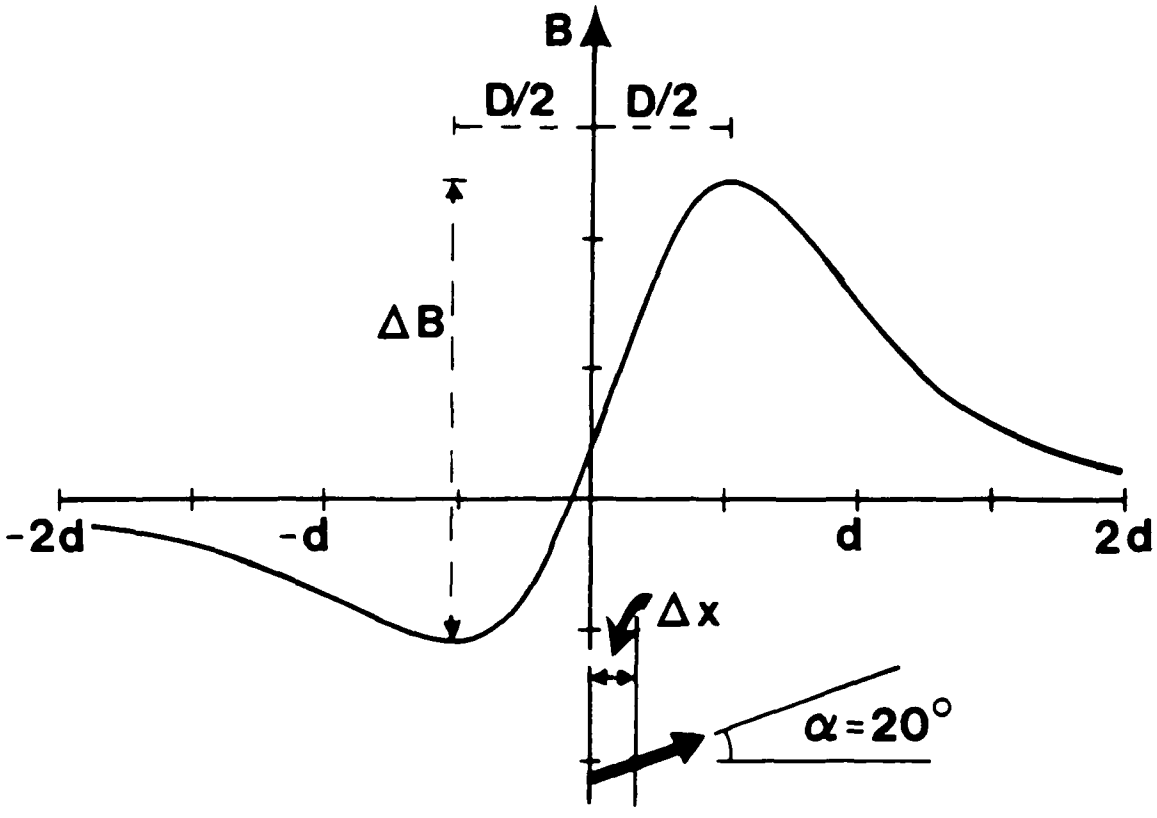

FIGURE 4

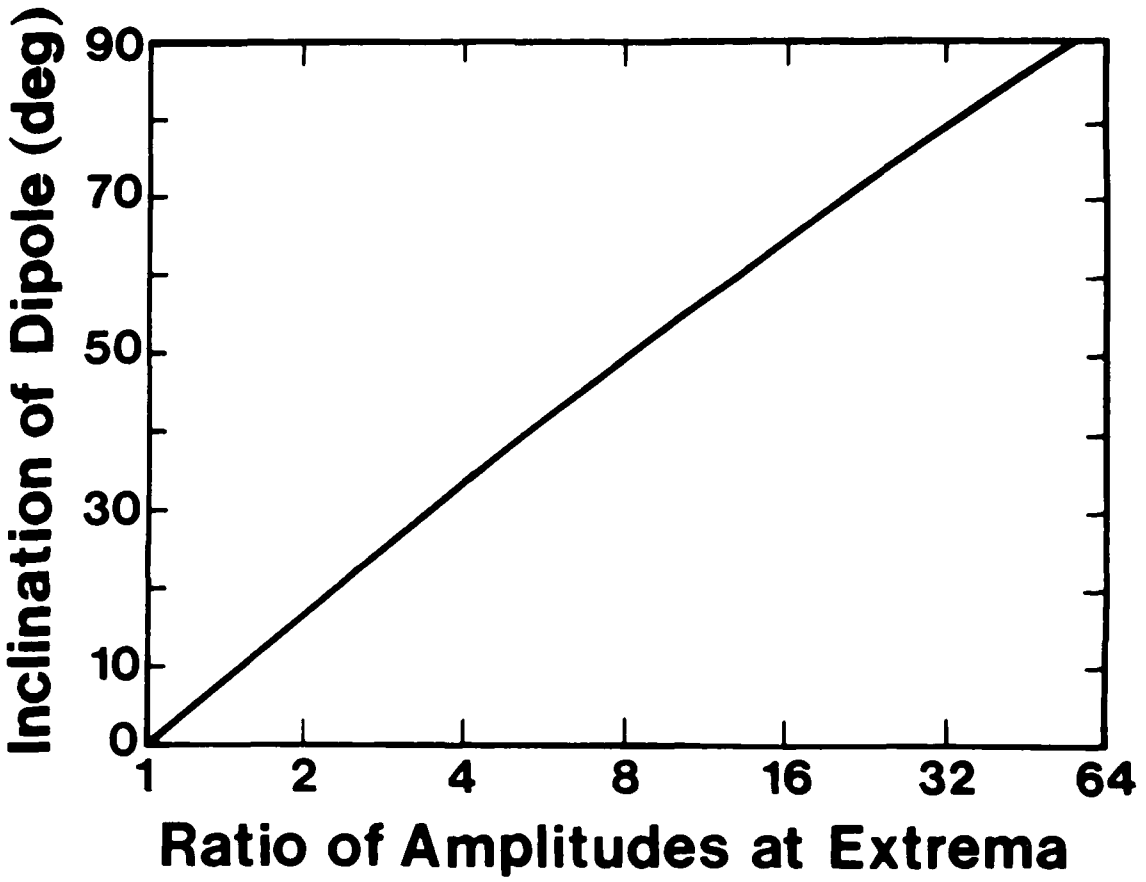
Inclination of Dipole (deg)
90
70
50
30
10
0
1
2
4
8
16
32
64
Ratio of Amplitudes at Extrema

FIGURE 5

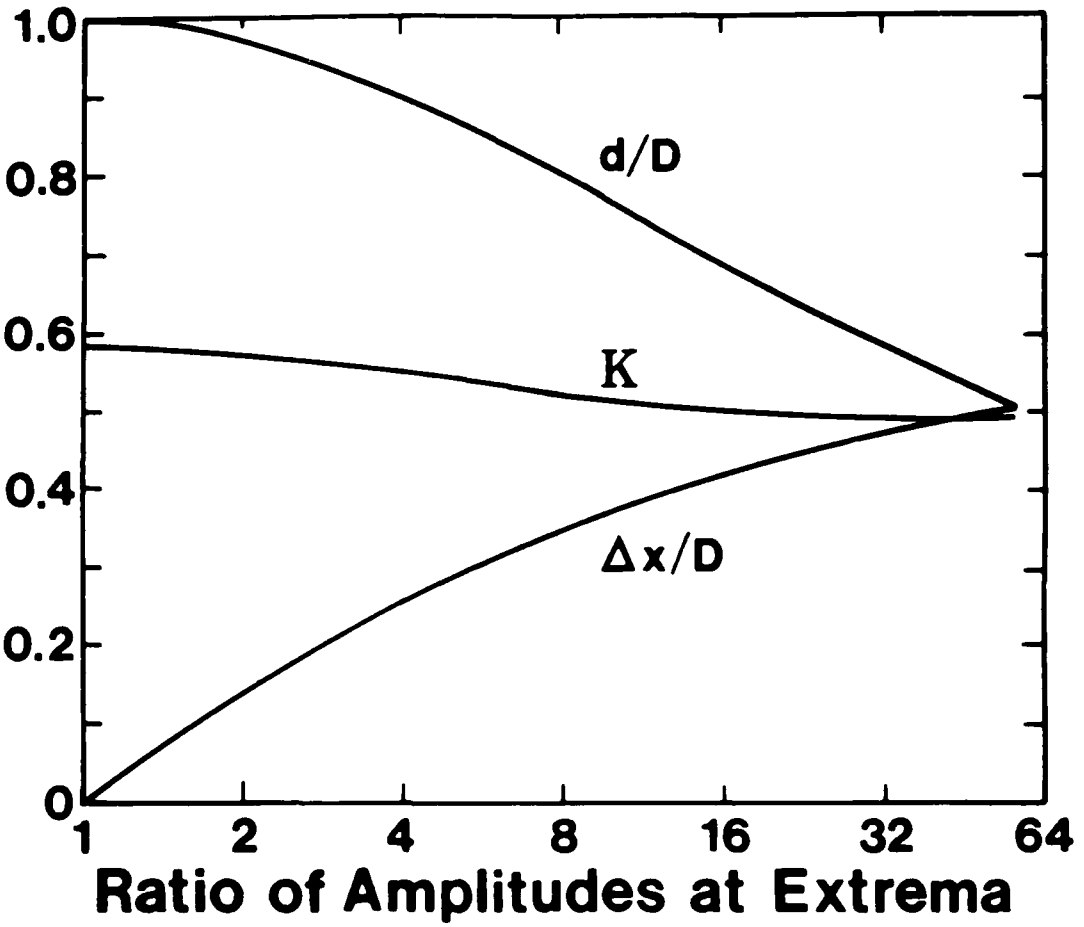
1.0
0.8
0.6
0.4
0.2
0
d/D
K
Δx/D
1
2
4
8
16
32
64
Ratio of Amplitudes at Extrema

FIGURE 6

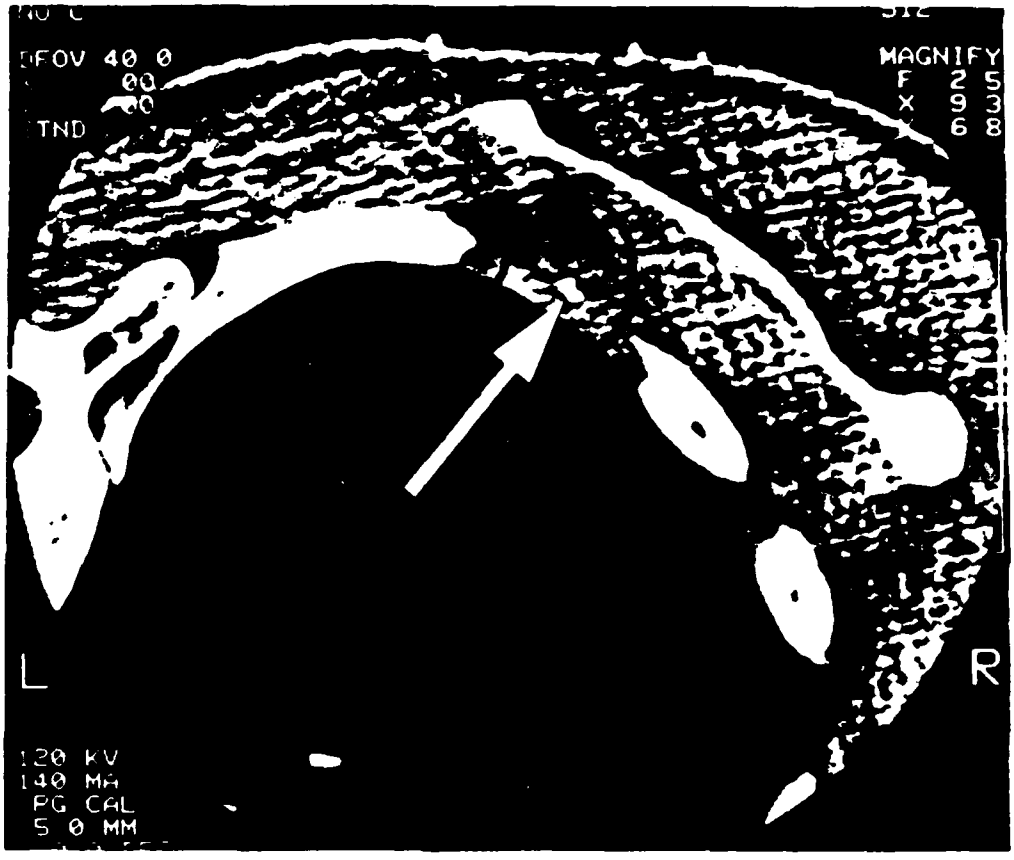
DFOV 40 0
00
00
TND
MAGNIFY
F 2 5
X 9 3
6 8
L
R
120 KV
140 MA
PG CAL
5 0 MM

FIGURE 7

END

DATE

FILM

DTIC

2—85